

Supporting Information

A well-defined lignin-based filler for tuning the mechanical properties of polymethyl methacrylate

Qingwen Cao,^a Qiong Wu,^a Lin Dai,^{*a,b} Xiaojun Shen,^{*c} and Chuanling Si^{*a}

^aTianjin Key Laboratory of Pulp and Paper, Tianjin University of Science and Technology, Tianjin 300457, China

^bState Key Laboratory of Pulp and Paper Engineering, South China University of Technology, Guangzhou 510640, China

^cState Key Laboratory of Catalysis, Dalian National Laboratory for Clean Energy, Dalian Institute of Chemical Physics, Chinese Academy of Sciences, Dalian 116023, China

*Corresponding author.

E-mail addresses: dailin@tust.edu.cn, shenxiaojun@iccas.ac.cn, sichli@tust.edu.cn

Table of Contents

1. Experimental Procedures

Materials

Fourier transform infrared (FT-IR) spectroscopy

Thermogravimetric analysis (TGA)

Light transmittance

2. Supplementary Figure

Fig. S1. Yields and FT-IR spectra of the lignin samples

Fig. S2. TGA and DTG curves of of PMMA and blends

Fig. S3. UV–Vis spectra of PMMA and blends

3. Supplementary Table

Table S1. The content of the hydroxyl and carboxyl groups of lignin

Table S2. Assignment of ^{13}C - ^1H cross-signals in 2 D HSQC spectra

Table S3. Comparison of the mechanical propertise of PMMA/*L-g*-PMMA and other PMMA/lignin materials.

Table S4. Values of stress, strain, and elastic modulus of the samples.

Table S5. Values of stress, strain, and elastic modulus of PMMA/*L*₁₅-*g*-PMMA.

4. References

1. Experimental Procedures

Materials. Alkaline lignin was supplied by Shandong Longlive Bio-technology Co., Ltd. (Jinan, China)¹⁻³. The manufacturing process for alkaline lignin used in this work was as follows: first, the corn cob was treated hydrothermally to remove the hemicelluloses. After further treatment with dilute alkaline, the effluent was separated and adjusted to acidic condition to precipitate the alkaline lignin, then dried at 50 °C vacua for 24 h prior to use.

Fourier transform infrared (FT-IR) spectroscopy. The chemical structures of the lignin fractions were analyzed by FT-IR spectroscopy (NICOLET iS5, Thermo Scientific) in the range of 4000–500 cm^{-1} with a resolution of 4 cm^{-1} and 32 scans.

Thermogravimetric analysis (TGA). TGA was carried on a Q50 thermogravimetric analyzer (TA instruments, USA). In this work, the mass of each sample was 3–4 mg and the carrier gas was nitrogen at a flow rate of 50 mL min^{-1} . Each sample was heated from 20 °C to 600 °C at 10 °C min^{-1} to record the TGA and differential thermogravimetric analysis (DTG) curves.

Light transmittance. Light transmittance of the blends was measured using a Varian ultraviolet–visible spectrophotometer (Cary 4000, USA). The scan was carried out from 200 nm to 800 nm at room temperature. The specimens were fabricated in the same way and the thickness was about 1.0 mm.

2. Supplementary Figure

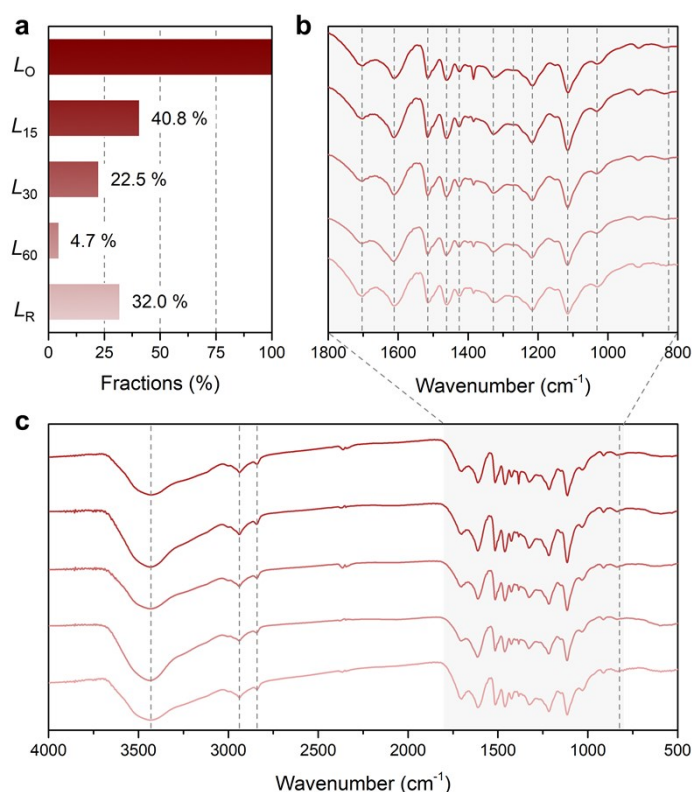


Fig. S1. Yields (a) and FT-IR spectra (b,c) of the lignin samples.

All the FT-IR spectra of lignin samples (L_0 , L_{15} , L_{30} , L_{60} , and L_R) show a broad absorption from 3100–3700 cm^{-1} revealing the vibrations of O–H in aliphatic structures (**Fig. 2b** and **c**).⁴ The peaks at 2937 cm^{-1} are attributed to the C–H symmetrical and asymmetric vibrations of C–H in methylene ($-\text{CH}_2$) and methyl ($-\text{CH}_3$) groups, and the peaks at 2839 cm^{-1} correspond to the methoxy ($-\text{O}-\text{CH}_3$) groups. The absorption peaks located in around 1703 cm^{-1} are attributed to the vibrations of conjugated ester and unconjugated carbonyl bonds formed by phenolic acids.⁵ The absorption peaks at 1610, 1516, and 1423 cm^{-1} reflect the vibrations of primary aromatic skeleton of lignin. Meanwhile, the absorption peaks at 1460 cm^{-1} correspond to the deformations of C–H and vibrations of aromatic skeleton. The peaks at 830 cm^{-1} are ascribed to aromatic out-of-plane C–H bending. The characteristic peaks of the syringyl (S) and guaiacyl (G) units in lignin macromolecules also showed at 1327/1217/1115 cm^{-1} and 1030 cm^{-1} , respectively. The stronger peak intensities of the S units indicate that the S units are the mainly structure in all the lignin samples.⁶

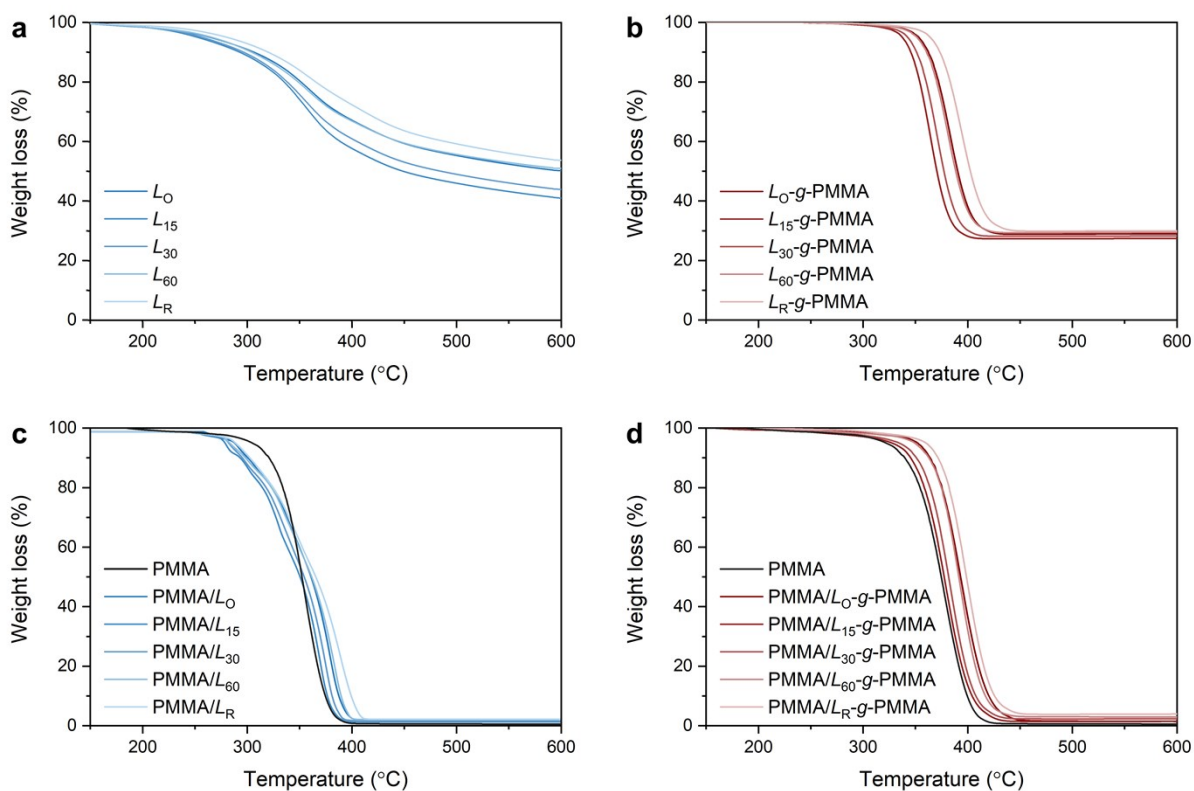


Fig. S2. TGA and DTG curves of of PMMA and blends.

Thermal stability of lignin fractions, *L-g*-PMMA, PMMA, and PMMA blends were investigated by TGA (**Fig. S2**). The initial decomposition temperature and the value of the residual mass of lignin fractions were increased with the degree of the fractionation. After graft modification by PMMA, the initial decomposition temperature of *L-g*-PMMA was obviously higher than that of PMMA, which could be due to the better thermal stability of PMMA side chains and their inhibitory effect on thermal degradation of copolymers.⁷ The thermal degradation processes of PMMA blends with lignin fractions and *L-g*-PMMA show similar tendencies as these lignin fillers.

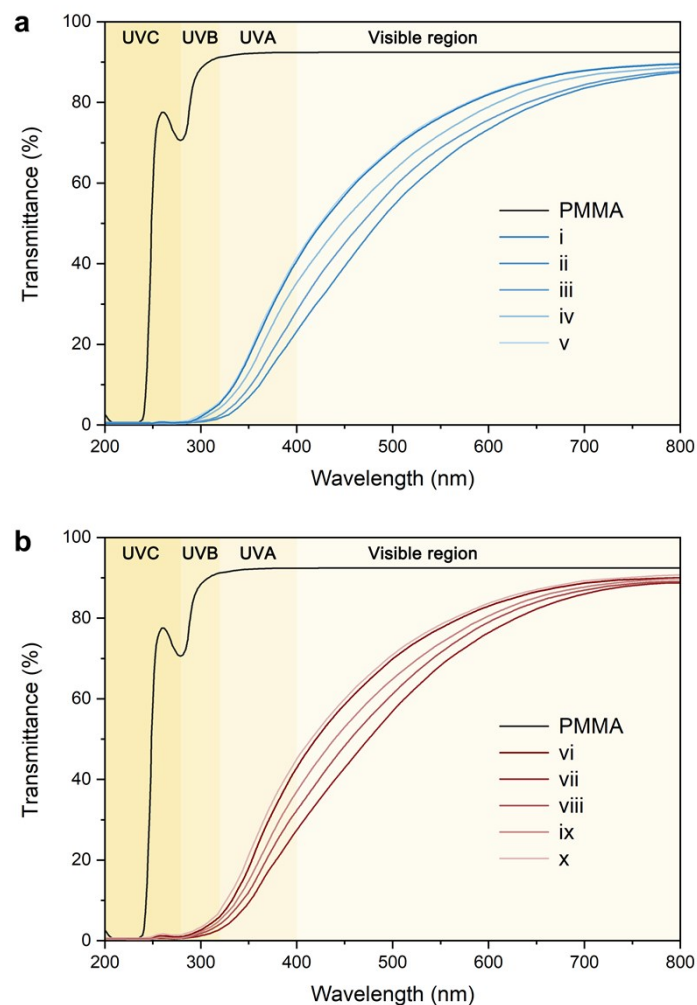


Fig. S3. UV–Vis spectra of PMMA and blends. (i) PMMA/ L_0 , (ii) PMMA/ L_{15} , (iii) PMMA/ L_{30} , (iv) PMMA/ L_{60} , (v) PMMA/ L_R , (vi) PMMA/ L_0 -g-PMMA, (vii) PMMA/ L_{15} -g-PMMA, (viii) PMMA/ L_{30} -g-PMMA, (ix) PMMA/ L_{60} -g-PMMA, (x) PMMA/ L_R -g-PMMA.

The optical properties of PMMA and blends were investigated by UV–vis spectroscopy (**Fig. S3**). The PMMA showed high transmittance both in the ultraviolet and visible regions. The lignin and lignin graft copolymer content PMMA blends show exhibit much better UV light barrier properties, which block about 100% of UVC (200~280 nm) and UVB (280~315 nm) and about 20% of UVA (315~400nm). The difference in optical properties is due to the difference in the structure (contents of aromatic rings and functional groups) and the color of lignin fractions.^{7, 8}

3. Supplementary Table

Table S1. The content of the hydroxyl and carboxyl groups of lignin.

Label	Contents (mmol g ⁻¹)				
	<i>L</i> ₀	<i>L</i> ₁₅	<i>L</i> ₃₀	<i>L</i> ₆₀	<i>L</i> _R
Aliphatic OH	0.26	0.37	0.34	0.14	0.12
Total S	1.02	1.19	1.12	0.99	0.55
Conph S	0.05	0.04	0.04	0.05	0.06
Nonph S	0.97	1.15	1.08	0.94	0.49
Total G	0.18	0.23	0.18	0.16	0.08
Conph G	0.03	0.02	0.03	0.03	0.04
Nonph G	0.15	0.21	0.15	0.13	0.04
Total phenolic OH	1.19	1.42	1.31	1.15	0.63
COOH	0.07	0.08	0.07	0.05	0.02
Total OH	1.45	1.79	1.65	1.29	0.75

^a Conph and Nonph mean the condensed and non-condensed phenolic –OH, respectively.

Table S2. Assignment of ^{13}C - ^1H cross-signals in 2 D HSQC spectra.

Label	$\delta_{\text{C}}/\delta_{\text{H}}$ (ppm)	Assignment
$-\text{OCH}_3$	55.7/3.74	C–H in methoxyls
A_γ	60.9/3.61 and 3.82	$\text{C}_\gamma\text{--H}_\gamma$ in $\beta\text{-O-4'}$ substructures (A)
B_γ	62.2/3.75	$\text{C}_\gamma\text{--H}_\gamma$ in phenylcoumaran substructures (B)
A_α	81.1/4.76	$\text{C}_\alpha\text{--H}_\alpha$ in $\beta\text{-O-4'}$ substructures (A)
A_β	71.0/ 4.18	$\text{C}_\beta\text{--H}_\beta$ in $\beta\text{-O-4'}$ substructures (A)
B_β	52.2/3.60	$\text{C}_\beta\text{--H}_\beta$ in phenylcoumaran substructures (B)
C_α	85.0/4.64	$\text{C}_\alpha\text{--H}_\alpha$ in resinol substructures (C)
C_β	54.2/3.06	$\text{C}_\beta\text{--H}_\beta$ in resinol substructures (C)
C_γ	70.6/3.79	$\text{C}_\gamma\text{--H}_\gamma$ in resinol substructures (C)
D_α	27.93/2.43	$\text{C}_\alpha\text{--H}_\alpha$ in secoisolariciresinol substructures (C)
D_β	34.79/2.02	$\text{C}_\beta\text{--H}_\beta$ in secoisolariciresinol substructures (C)
$\text{S}_{2,6}$	104.1/6.69	$\text{C}_{2,6}\text{--H}_{2,6}$ in syringyl (S)
$\text{S}'_{2,6}$	106.3/7.32	$\text{C}_{2,6}\text{--H}_{2,6}$ in oxidized syringyl (S')
G_2	110.6/7.0	$\text{C}_2\text{--H}_2$ in guaiacyl (G)
G_5/G_6	115.1/6.64, 6.76, and 6.85	$\text{C}_5\text{--H}_5$ and $\text{C}_6\text{--H}_6$ in guaiacyl (G)
$\text{H}_{3,5}$	112.3/6.61	$\text{C}_{3,5}\text{--H}_{3,5}$ <i>p</i> -hydroxyphenyl (H)
$\text{H}_{2,6}$	123.6/7.38	$\text{C}_{2,6}\text{--H}_{2,6}$ <i>p</i> -hydroxyphenyl (H)

Table S3. Comparison of the mechanical propertise of PMMA/*L-g*-PMMA and other PMMA/lignin materials.

Label	Form	Raw lignin	Content of lignin (wt%)	Stress (MPa)	Strain (%)	Modulus (GPa)	Ref.
PMMA-L-1	Blend	Kraft lignin	1	70.92 ± 5.17	4.97 ± 0.79	0.27	9
PMMA-L-2	Blend	Kraft lignin	3	57.63 ± 5.54	5.15 ± 0.61	0.26	9
PMMA-L-3	Blend	Kraft lignin	5	39.09 ± 1.38	7.73 ± 1.35	0.25	9
Lignin22.1PMMA401	Copolymer	Alkaline lignin	22.1	~5	~20	0.056	10
Lignin8.3PMMA388	Copolymer	Alkaline lignin	8.3	~10	~60	0.046	10
Lignin4.5PMMA323	Copolymer	Alkaline lignin	4.5	~7	~70	0.055	10
LM30	Copolymer	Alkaline lignin	46.1	–	–	–	11
LM50	Copolymer	Alkaline lignin	31.4	–	–	–	11
LM70	Copolymer	Alkaline lignin	6.4	–	–	–	11
LM100	Copolymer	Alkaline lignin	5.6	–	–	–	11
PMMA/ Lignin-8MMA388	Blend	Alkaline lignin	0.5	~16	~9	~0.6	12
PMMA/ Lignin-8MMA388	Blend	Alkaline lignin	1	~23	~12	~0.7	12
PMMA/ Lignin-8MMA388	Blend	Alkaline lignin	2	~12	~18	~0.2	12
PMMA+AL 1%	Blend	Acetosolv lignin	1	–	–	2.1	13
PMMA+AL 5%	Blend	Acetosolv lignin	5	–	–	1.9	13
PMMA+AAL 1%	Blend	Acetylated acetosolv lignin	1	–	–	2.0	13
PMMA+AAL 5%	Blend	Acetylated acetosolv lignin	5	–	–	1.9	13
PMMA/1.0%WCSAL	Blend	Coconut shell	1	–	–	1.7	14

		acetosolv lignin					
PMMA/1.0%ACT-F	Blend	Acetone soluble WCSAL	1	–	–	1.3	¹⁴
PMMA/1.0%EtOH-F	Blend	Ethanolic soluble WCSAL	1	–	–	1.6	¹⁴
OL0.4-g-PMMA	Copolymer	Organosolv lignin	0.4	54.1 ± 1.2	6.0 ± 1.2	~1.7	⁷
OL2.1-g-PMMA	Copolymer	Organosolv lignin	2.1	66.2 ± 2.2	6.1 ± 0.8	~1.7	⁷
OL8.7-g-PMMA	Copolymer	Organosolv lignin	8.7	47.4 ± 2.0	6.5 ± 0.4	~1.6	⁷
OL13.8-g-PMMA	Copolymer	Organosolv lignin	13.8	51.4 ± 1.2	6.7 ± 1.5	~1.5	⁷
OL20.1-g-PMMA	Copolymer	Organosolv lignin	20.1	57.1 ± 1.9	6.0 ± 0.5	~1.6	⁷
PMMA/ <i>L</i> ₁₅ -g-PMMA (This work)	Blend	Alkaline lignin	1	124.96 ± 4.43	2.46 ± 0.05	5.08 ± 0.23	

Table S4. Values of stress, strain, and elastic modulus of the samples.

Label	Stress (MPa)	Strain (%)	Modulus (GPa)
PMMA	65.02 ± 6.25	2.26 ± 0.07	3.05 ± 0.20
PMMA/ <i>L</i> ₀	52.91 ± 10.32	2.29 ± 0.10	2.49 ± 0.38
PMMA/ <i>L</i> ₁₅	55.43 ± 7.98	2.30 ± 0.06	2.62 ± 0.36
PMMA/ <i>L</i> ₃₀	72.27 ± 6.41	2.72 ± 0.07	3.29 ± 0.26
PMMA/ <i>L</i> ₆₀	70.07 ± 7.52	2.85 ± 0.06	3.14 ± 0.34
PMMA/ <i>L</i> _R	35.15 ± 15.86	3.31 ± 0.13	1.29 ± 0.54
PMMA/ <i>L</i> ₀ -g-PMMA	112.37 ± 6.95	2.56 ± 0.07	4.49 ± 0.29
PMMA/ <i>L</i> ₁₅ -g-PMMA	124.96 ± 4.43	2.46 ± 0.05	5.08 ± 0.23
PMMA/ <i>L</i> ₃₀ -g-PMMA	122.73 ± 6.11	2.71 ± 0.04	4.69 ± 0.22
PMMA/ <i>L</i> ₆₀ -g-PMMA	107.72 ± 5.26	2.97 ± 0.05	3.80 ± 0.19
PMMA/ <i>L</i> _R -g-PMMA	64.45 ± 8.07	3.04 ± 0.10	2.26 ± 0.28

Table S5. Values of stress, strain, and elastic modulus of PMMA/*L*₁₅-g-PMMA.

<i>L</i> ₁₅ -g-PMMA (wt%)	Stress (MPa)	Strain (%)	Modulus (GPa)
0	65.02 ± 6.25	2.26 ± 0.07	3.05 ± 0.20
0.5	105.31 ± 4.59	2.37 ± 0.06	4.15 ± 0.22
1.0	124.96 ± 4.43	2.46 ± 0.05	5.08 ± 0.23
1.5	96.82 ± 4.96	2.41 ± 0.05	3.98 ± 0.26
2.0	80.25 ± 5.25	2.32 ± 0.05	3.61 ± 0.28

4. References:

1. S. Yang, J.-L. Wen, T.-Q. Yuan and R.-C. Sun, *RSC Advances*, 2014, 4, 57996-58004.
2. B. Wang, D. Sun, H.-M. Wang, T.-Q. Yuan and R.-C. Sun, *ACS Sustainable Chemistry & Engineering*, 2019, 7, 2658-2666.
3. Y. Zhang, J.-Q. Wu, H. Li, T.-Q. Yuan, Y.-Y. Wang and R.-C. Sun, *ACS Sustainable Chemistry & Engineering*, 2017, 5, 7269-7277.
4. A. Toledano, L. Serrano, A. Garcia, I. Mondragon and J. Labidi, *Chemical Engineering Journal*, 2010, 157, 93-99.
5. G. Wang and H. Chen, *Separation and Purification Technology*, 2013, 120, 402-409.
6. I. de Menezes Nogueira, F. Avelino, D. R. de Oliveira, N. F. Souza, M. F. Rosa, S. E. Mazzetto and D. Lomonaco, *International Journal of Biological Macromolecules*, 2019, 122, 1163-1172.
7. W. Huang, M. Wu, W. Liu, Z. Hua, Z. Wang and L. Zhou, *Applied Surface Science*, 2019, 475, 302-311.
8. J. Wang, Y. Deng, Y. Qian, X. Qiu, Y. Ren and D. Yang, *Green Chemistry*, 2016, 18, 695-699.
9. K. Soygun, S. Şimşek, E. Yılmaz and G. Bolayır, *Advances in Materials Science and Engineering*, 2013, 2013, 435260.
10. S. L. Hilburg, A. N. Elder, H. Chung, R. L. Ferebee, M. R. Bockstaller and N. R. Washburn, *Polymer*, 2014, 55, 995-1003.
11. D. Kai, S. Jiang, Z. W. Low and X. J. Loh, *Journal of Materials Chemistry B*, 2015, 3, 6194-6204.
12. T. Shah, C. Gupta, R. L. Ferebee, M. R. Bockstaller and N. R. Washburn, *Polymer*, 2015, 72, 406-412.
13. D. R. de Oliveira, I. d. M. Nogueira, F. J. N. Maia, M. F. Rosa, S. E. Mazzetto and D. Lomonaco, *Journal of Applied Polymer Science*, 2017, 134, 45498.
14. F. Avelino, D. R. de Oliveira, S. E. Mazzetto and D. Lomonaco, *International Journal of Biological Macromolecules*, 2019, 125, 171-180.